INTERNATIONAL JOURNAL OF
NUMERICAL ANALYSIS AND MODELING
Volume 9, Number 3, Pages 529–542

NUMERICAL SIMULATION OF RESERVOIR MULTICOMPONENT FLUID MIXING

ZHANGXIN CHEN AND HONGSEN CHEN

(Communicated by Kenneth H. Karlsen)

This paper is dedicated to the memory of Professor Magne S. Espedal.

Abstract. This paper presents numerical results on the development of compositional fluid mixing simulators in porous media. These simulators integrate geological processes (source rock maturation, hydrocarbon generation, migration, charge/filling, etc.) and reservoir processes (fluid mixing through Darcy's flow, advection, and diffusion, gravity segregation, etc.). The model governing equations are written with a proper choice of solution variables so that numerical mass conservation is preserved for all chemical components. The approximation procedure uses the finite volume method for space discretization, the backward Euler scheme in time, and an adaptive time stepping technique. The traditional simulator for solving the isothermal gravity/chemical equilibrium problem is deduced as a special example of the simulators presented here. Extensive numerical experiments are given to show segregation and instability effects for multiple components.

Key words. compositional gradients, reservoir simulation, fluid mixing, advection, diffusion, gravity segregation, numerical experiment, instability

1. Introduction

Compositional variations with depth have been observed in hydrocarbon reservoirs. These variations result from a variety of sources and typically indicate nonequilibrium states. They can be observed in systems in equilibrium when chemical potential gradients are balanced by gravitational potential gradients [8, 10, 13, 14, 21, 22, 24]. Temperature gradients can also contribute to compositional variations. Compositional variations in hydrocarbon reservoirs play an important role in reservoir delineation. The ability to forecast horizontal compositional variations helps the petroleum engineer to determine whether a given pair of producing wells drain the same reservoir, for example. Their other important applications include the study of the interplay of heterogeneity, advection, diffusion, gravity, viscosity, reservoir segmentation, and other forces that may affect the distribution of chemical components in reservoirs [4, 15].

In particular, the application to reservoir segmentation has increasingly become important due to exploration demands of new energy resources. Common assumptions are that there is a high chance of reservoir connectivity if

- Reservoir fluids are in pressure equilibrium;
- Fluids have similar or continuous PVT (pressure, volume, and temperature) properties;
- Fluids have similar geochemical compositions;

Received by the editors February 20, 2011 and, in revised form, May 14, 2011.
2000 *Mathematics Subject Classification.* 35Q10, 65N30, 76D05.
This research was supported in part NSERC/AERI/Foundation CMG Chair and iCORE Chair Funds in Reservoir Simulation.

- There are no significant changes in lithological characteristics from core and well log interpretation;
- Seismic reflectors are continuous;
- There is a common hydrocarbon-water contact.

Thus one needs to understand how similarities and differences can be interpreted from these diverse data sets when assessing reservoir segmentation. On one hand, multiple processes that affect fluid properties include reservoir charge/filling, fluid mixing through Darcy's flow, advection, and diffusion, gravity segregation, biodegradation, fractionation, and differential leakage of gas vs. oil. On the other hand, distinct time scales (key to understanding the relative significance of fluid data to reservoir segmentation studies) occur for different processes:

- Charge/filling of reservoirs: geological time–several millions of years;
- Biodegradation: thousands to hundreds of thousand of years;
- Molecular diffusion: 1 to 100 million years;
- Pressure diffusion: hundreds or even thousands of years;
- Convective flow: thousands to million years.

Therefore, one needs process-driven simulators to isolate the effects of each of these processes to evaluate reservoir fluid data in the interpretation of compartmentalization. We have been developing a software package that will integrate geological processes (source rock maturation, hydrocarbon generation, migration, charge/filling, etc.) and reservoir processes (fluid mixing through Darcy's flow, advection, and diffusion, gravity segregation, etc.). In the current paper instability problems (fingering phenomena) due to the interplay of advection, diffusion, and gravity are especially studied for multiple components. The literature is rich in the study of instability problems [9, 20, 23]. However, most of the studies dealt with viscous fingering and gravity segregation for two fluid components in a different setting.

The model equations governing the flow and transport of chemical components are written with a proper choice of solution variables so that numerical mass conservation is preserved for all these components. The approximation procedure here uses the finite volume method for space discretization, the backward Euler scheme in time, and an adaptive time stepping technique. Extensive numerical experiments are given to show segregation and instability effects for multiple components.

The rest of the paper is organized as follows. In the next section, we present the governing differential equations. Then, in the third section, we show that Gibbs' formulation can be treated as a special example of the mathematical formulation developed here. In the fourth section, the choice of the primary variables is given, and remarks about the approximation procedure used are made. In the fifth section extensive numerical experiments are presented. Finally, we draw several concluding remarks in the last section. Nomenclature is provided at the end of this paper.

2. Governing Differential Equations

We consider a gas or liquid phase that consists of N_c chemical species, where there is no viscous dissipation and chemical reaction and the only external force is due to gravity. Conservation of mass of each component in the fluid mixture is

$$\frac{\partial(\phi x_i \xi)}{\partial t} = -\nabla \cdot (x_i \xi \mathbf{u} + \mathbf{J}_i) + q_i, \qquad i = 1, 2, \ldots, N_c, \tag{2.1}$$

where ϕ is the porosity, ξ and $\mathbf{u}$ are the fluid molar density and velocity, and x_i, q_i, and $\mathbf{J}_i$ are the mole fraction, the source/sink term, and the diffusive mass flux

of the ith component, respectively. Darcy's law for the fluid is

$$\mathbf{u} = -\frac{1}{\mu}\mathbf{k}\left(\nabla p - \rho g \nabla z\right), \tag{2.2}$$

where $\mathbf{k}$ is the permeability tensor, μ, p, and ρ are the fluid viscosity, pressure, and mass density, respectively, g is the gravitational constant, and z is the depth.

The equation of conservation of energy is

$$\frac{\partial(\rho_b c_b T)}{\partial t} + \nabla \cdot (\rho c_p u T) = \nabla \cdot (k_T \nabla T) + q_T, \tag{2.3}$$

where T, ρ_b, c_b, c_p, k_T, and q_T are the temperature, bulk density, bulk specific heat capacity, heat capacity of the fluid, fluid/rock thermal conductivity, and source/sink term, respectively. For more details for these equations, the reader can refer to [1, 2, 5].

The unknowns in equations (2.1)–(2.3) are the mole fractions $\mathbf{x} = (x_1, x_2, \ldots, x_{N_c})$, pressure p, and temperature T. The mole fraction balance implies

$$\sum_{i=1}^{N_c} x_i = 1. \tag{2.4}$$

The fluid viscosity has the following dependence:

$$\mu = \mu(p, T, x_1, x_2, \ldots, x_{N_c}),$$

which can be obtained, for example, from the correlation of Lohrenz et al. [12] with the input data: the critical pressure, critical temperature, critical volume, and molecular weight of each component. The molar density

$$\xi = \xi(p, T, x_1, x_2, \ldots, x_{N_c})$$

can be calculated using the equations of state of Peng-Robinson or Redlich-Kwong-Soave. The method of volume translation is widely used for correcting volumetric deficiencies of the original PR [19] and RKS [18] equations. The fluid mass density is calculated as follows:

$$\rho = \xi W \equiv \xi \sum_{i=1}^{N_c} x_i W_i, \tag{2.5}$$

where W is the total molecular weight and W_i is the molecular weight of the ith component. Set

$$\mathbf{J} = (\mathbf{J}_1, \mathbf{J}_2, \ldots, \mathbf{J}_{N_c})^t,$$

where the superscript t indicates the transpose of a vector or matrix. Then the diffusive mass flux of each component in equation (2.1) takes the form

$$\mathbf{J}_i = -\phi\xi\left(\sum_j \mathbf{D}_{ij}^M \nabla x_j + \mathbf{D}_i^T \nabla T + \mathbf{D}_i^p \nabla p\right), \tag{2.6}$$

where $\mathbf{D}_{ij}^M$, $\mathbf{D}_i^T$, and $\mathbf{D}_i^p$ are the molecular, thermal (the Soret effect), and pressure (gravity segregation) diffusions of component i [7], respectively. Note that the diffusive fluxes satisfy

$$\sum_{i=1}^{N_c} \mathbf{J}_i = \mathbf{0}.$$

Following [7], each $\mathbf{J}_i$ is given by, $i = 1, 2, \ldots, N_c - 1$,

(2.7)
$$\mathbf{J}_i = -\phi\xi a_{iN_c} D_{iN_c} \Bigg\{ \frac{W_i x_i}{L_{ii}} \sum_{k=1}^{N_c-1} L_{ik} \sum_{j=1}^{N_c-1} \frac{W_j x_j + W_{N_c} x_{N_c} \delta_{jk}}{W_j} \sum_{l=1}^{N_c-1} \frac{\partial \ln f_j}{\partial x_l} \nabla x_l + \frac{W k_{Ti}}{T} \nabla T + \frac{W_i x_i}{RTL_{ii}} \sum_{k=1}^{N_c-1} L_{ik} \left(\sum_{j=1}^{N_c-1} x_j v_j + \frac{W_{N_c} x_{N_c}}{W_k} v_k - \frac{1}{\xi} \right) \nabla p \Bigg\},$$

where L_{ik} is a phenomenological coefficient, δ_{jk} denotes the Kronecker symbol, R is the gas constant, f_i and v_i are the fugacity and partial molar volume of component i, and the coefficients a_{iN_c}, D_{iN_c}, and k_{Ti} (the thermal diffusion ratio) are defined by, $i = 1, 2, \ldots, N_c - 1$,

$$a_{iN_c} = \frac{W_i W_{N_c}}{W^2}, \quad D_{iN_c} = \frac{W^2 R L_{ii}}{\xi W_i^2 W_{N_c}^2 x_i x_{N_c}}, \quad k_{Ti} = \frac{W_i x_i W_{N_c} x_{N_c} L_i'}{WRTL_{ii}} \equiv \alpha_{Ti} x_i x_{N_c},$$

with L_i' being another phenomenological coefficient and α_{Ti} called the thermal diffusion factor of component i. For information on the phenomenological coefficients L_{ik} and L_i', the reader may refer to [16, 17].

3. Isothermal Gravity/Chemical Equilibrium

The formulation for computing compositional variations under gravity for an isothermal system was first given by Gibbs [8]. In this section we show that Gibbs' formulation for this type of system can be treated as a special example of the mathematical formulation developed in the previous section. The constraint of chemical equilibrium is

$$d\mu_i + W_i g dz = 0, \qquad i = 1, 2, \ldots, N_c, \tag{3.1}$$

$$d\mu_i + W_i g dz = Q_i \frac{dT}{T}, \qquad i = 1, 2, \ldots, N_c, \tag{3.2}$$

where μ_i is the chemical potential of component i. Equations (2.4) and (3.1) provide compositions $(x_1, x_2, \ldots, x_{N_c})$ and pressure p at any depth z once they are specified at a reference depth. An interesting fact is that the Gibbs equation (3.1) can be obtained using (2.7) and the condition of mechanical equilibrium

$$dp = -\rho g dz. \tag{3.3}$$

For an isothermal system at the steady state,

$$\mathbf{J}_i = \mathbf{0}, \qquad i = 1, 2, \ldots, N_c.$$

Applying (2.7) in the z-direction, we see that

$$\sum_{k=1}^{N_c-1} L_{ik} \sum_{j=1}^{N_c-1} \frac{W_j x_j + W_{N_c} x_{N_c} \delta_{jk}}{W_j} \sum_{l=1}^{N_c-1} \frac{\partial \ln f_j}{\partial x_l} \frac{dx_l}{dz} + \frac{1}{RT} \sum_{k=1}^{N_c-1} L_{ik} \left(\sum_{j=1}^{N_c-1} x_j v_j + \frac{W_{N_c} x_{N_c}}{W_k} v_k - \frac{1}{\xi} \right) \frac{dp}{dz} = 0. \tag{3.4}$$

Note that this equation must hold for any combination of the compositions $(x_1, x_2, \ldots, x_{N_c})$. In particular, for a fixed $j = k$ and $x_m = 0$ for all m's except possibly for $m = j$ or N_c, equation (3.4) reduces to

$$\frac{W_j x_j + W_{N_c} x_{N_c}}{W_j} \sum_{l=1}^{N_c-1} \frac{\partial \ln f_j}{\partial x_l} \frac{dx_l}{dz} + \frac{1}{RT} \left(x_j v_j + \frac{W_{N_c} x_{N_c}}{W_j} v_j - \frac{1}{\xi} \right) \frac{dp}{dz} = 0, \tag{3.5}$$

which, together with equations (2.5) and (3.3), implies

$$RT \sum_{l=1}^{N_c-1} \frac{\partial \ln f_j}{\partial x_l} \frac{dx_l}{dz} - g(\rho v_j - W_j) = 0, \qquad i = 1, 2, \ldots, N_c - 1. \tag{3.6}$$

This equation is exactly the condition (3.1) by noting that

$$\frac{\partial \mu_j}{\partial x_l} = RT \frac{\partial \ln f_j}{\partial x_l}, \quad \frac{\partial \mu_j}{\partial p} = v_j.$$

We remark that the chemical equilibrium constraint (3.1) (segregation equation) holds only for an isothermal system. For nonisothermal systems, this constraint is no longer valid because of nonzero entropy production. Furthermore, transience is not solved so there is no driving force, as noted earlier. In this paper we will use the more general, transient governing equations developed in the previous section. These equations include the effects of advection, diffusion, and gravity segregation.

4. Choice of Primary Variables and Numerical Methods

Traditionally, mole fractions $\mathbf{x} = (x_1, x_2, \ldots, x_{N_c})$ and pressure p are chosen to be the primary variables (primary unknowns). Then the time discretization requires that the time derivative term be rewritten as follows:

$$\phi \frac{\partial (x_i \xi)}{\partial t} = \phi \left(\xi + x_i \frac{\partial \xi}{\partial x_i} \right) \frac{\partial x_i}{\partial t} + \phi x_i \frac{\partial \xi}{\partial p} \frac{\partial p}{\partial t}.$$

In numerical experiments we have observed that this formula causes a numerical error in mass conservation. To conserve mass numerically, we choose the primal variables to be the partial molar densities $r_i = x_i \xi$, the pressure p, and the temperature T. From equation (2.1), the former satisfies

$$\frac{\partial (\phi r_i)}{\partial t} = -\nabla \cdot (r_i \mathbf{u} + \mathbf{J}_i) + q_i, \qquad i = 1, 2, \ldots, N_c. \tag{4.1}$$

The molar density ξ is evaluated from the equations of state. After ξ and r_i are obtained, the mole fractions x_i are computed from $x_i = r_i/\xi$, $i = 1, 2, \ldots, N_c$.

The approximation procedure uses the finite volume method for space discretization, the backward Euler scheme in time, and a sequential implicit solution scheme for solving the partial molar density, pressure, and temperature equations. The pressure equation can be obtained from the mass conservation equations (2.1) and the mole fraction balance equation (2.4) [1, 2]. Furthermore, a simple algorithm for adaptive time stepping is used in the selection of time steps. It attempts to use as large time steps as possible while accuracy is preserved [2]. The main parameters that affect the choice of time steps are the maximum allowable pressure, partial molar density, and temperature changes, their minimum time steps, and their maximum allowable variations [2]. Both Dirichlet and/or Neumann boundary conditions and initial conditions can be specified for pressure, partial molar densities, and temperature.

5. Numerical Experiments

In this section numerical results are presented. The interplay of advection, diffusion, and gravity segregation was reported in [4]; here special attention is paid to the study of gravity segregation for multiple components and their instability. Hence the temperature T is fixed in all three examples. In the first two examples, we study a mixture of binary components, and in the final example a mixture of six components. The first example focuses on the study of compositional equilibrium, the second one on the instability study for two components using the present methodology, and the last on instability for multiple components.

5.1. Example 1A. A rectangular reservoir is initially filled with two fluid components (Fig. 5.1). The left-hand half of this reservoir is filled with a heavy component and the right-hand half with a light component. The two parts of the reservoir have a density difference, which results in the light component moving up to the top half of the reservoir and the heavy component to the bottom half until equilibrium is reached in a horizontal position (Fig. 5.2). No-flow boundary conditions are used for the pressure and partial molar density equations. The reservoir length is 1,000 m, and the rock porosity is 0.2.

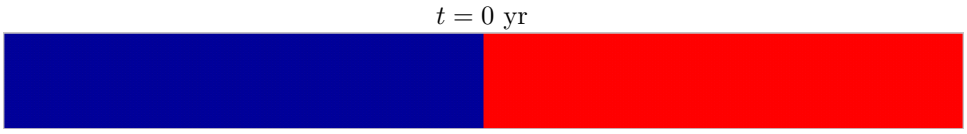

FIGURE 5.1. Initial mole fraction of Example 1.

The simulation results match very well with the analytic solution

$$\left(\frac{2x}{H}\right)^2 = \frac{16}{3}F^2\frac{k_h}{k_v}\frac{(t/t_0)^2}{1+t/t_0}, \quad t_0 = \frac{4}{3}\frac{\phi H\mu F}{k_v g\Delta\rho},$$

where

$k_h = 100$ (md)	:	the horizontal permeability;
$k_v = 100$ (md)	:	the vertical permeability;
$H = 100$ (m)	:	the height;
$\mu = 1$ (cp)	:	the fluid mixture viscosity;
$F = 1$	:	a function of the viscosity;
$\Delta\rho = 10$ kg/m^3	:	the density difference,
$2x$ (m)	:	the width of the mixing interface.

For this example we have observed that the mass conservation error is within 0.0024% after 50,000 yr (see Fig. 5.3).

5.2. Example 1B. When the molecular diffusion, gravitational diffusion, and natural convection are all present, it takes much time to attain compositional equilibrium. With the same set of data and meshes as above, a molecular diffusion constant is now introduced: 1.7×10^{-10}m^2/s. For the resulting problem, the simulation predicts a total equilibrated system at about 400 Myr (see Figs. 5.4 and 5.5, where the mole fractions of the heavy component are shown and the magnitude of the color is given in the last figure of Fig. 5.4).

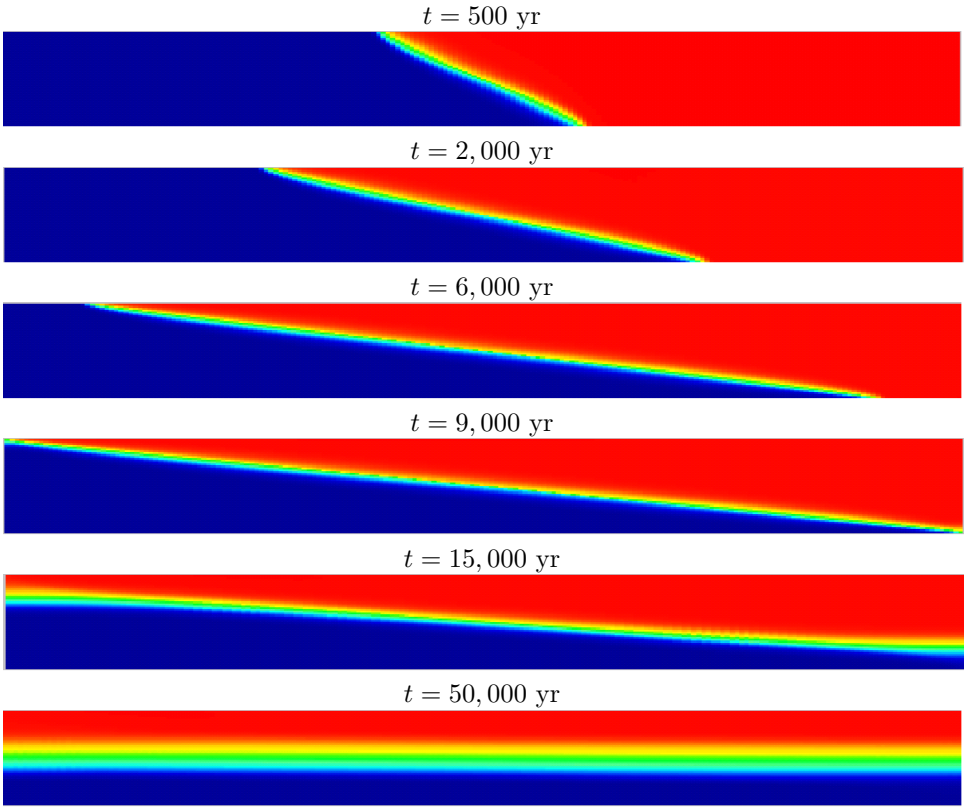

FIGURE 5.2. Mole fractions of Example 1 at different times.

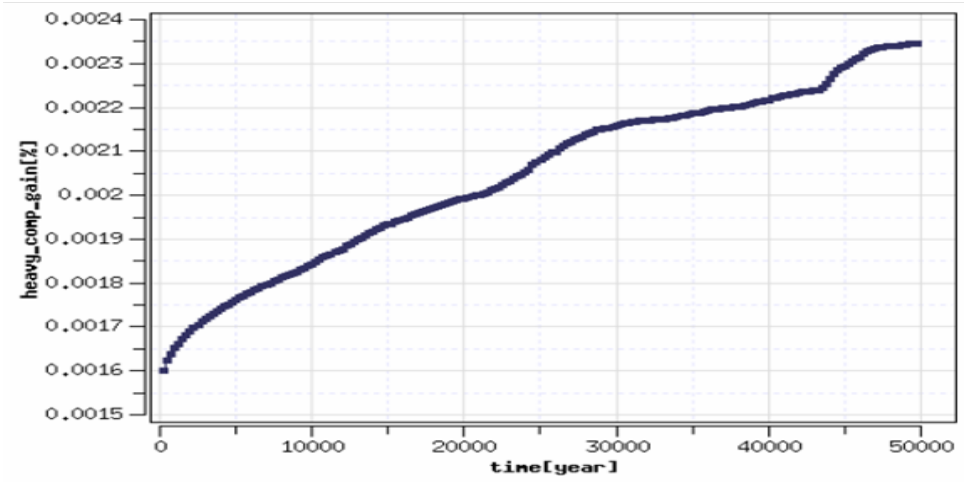

FIGURE 5.3. Mass conservation error of Example 1.

5.3. Example 2. As another example we consider a non-zero boundary condition for the mole fraction equations. The boundary condition for the pressure equation is a zero flux (no flow). The boundary conditions for the mole fraction equations

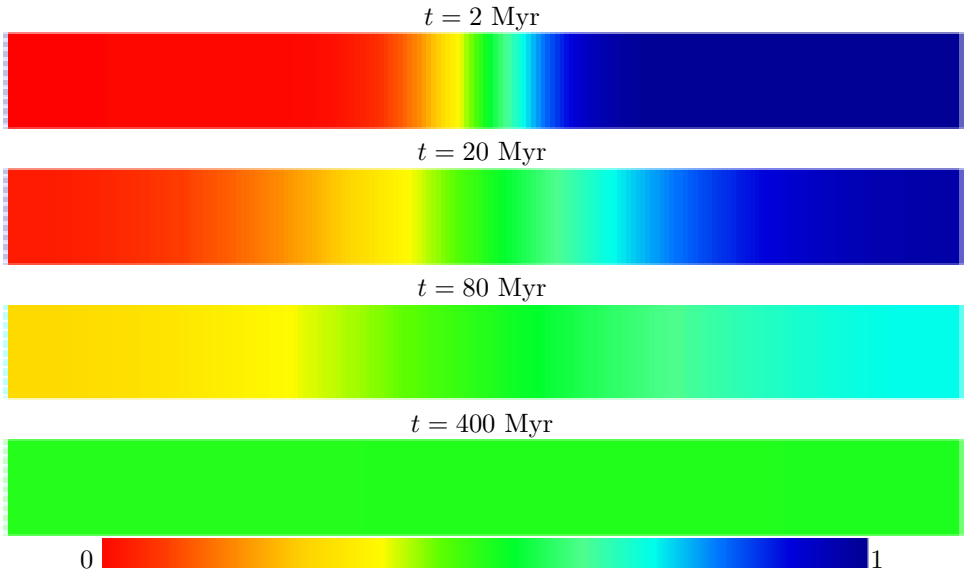

FIGURE 5.4. Equilibrium time of Example 1.

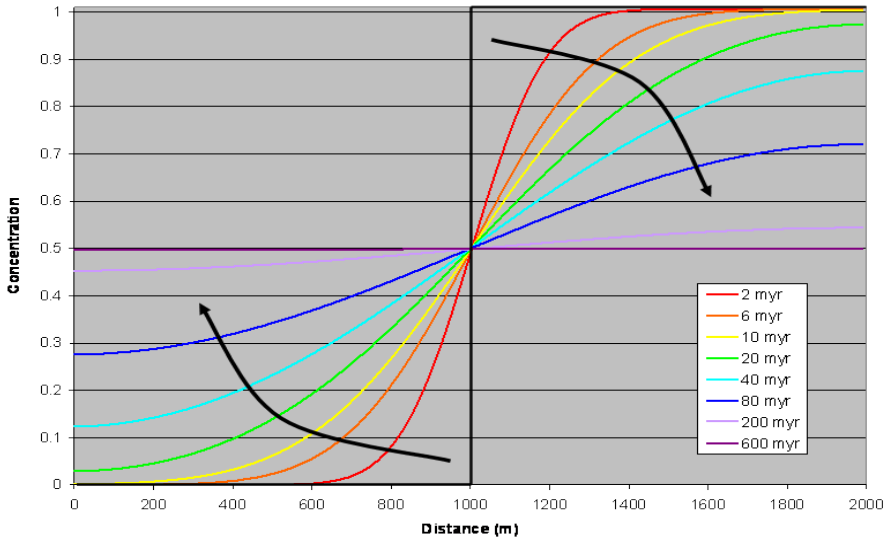

FIGURE 5.5. Reaching equilibrium of Example 1.

are a zero flux on the side vertical boundaries and constant fractions on the top and bottom boundaries. The molar density is a linear function of a mole fraction:

$$\xi = \xi_{max} + (\xi_{min} - \xi_{max})x_1.$$

Let Ra_c be the chemical Rayleigh number defined by [6, 11]

$$Ra_c = \frac{gk\beta\Delta x_1 \bar{\xi} H}{D\mu},$$

with $\beta = \dfrac{1}{\bar{\xi}} \dfrac{\partial \xi}{\partial x_1}$ and $\bar{\xi} = 0.5(\xi_{min} + \xi_{max})$.

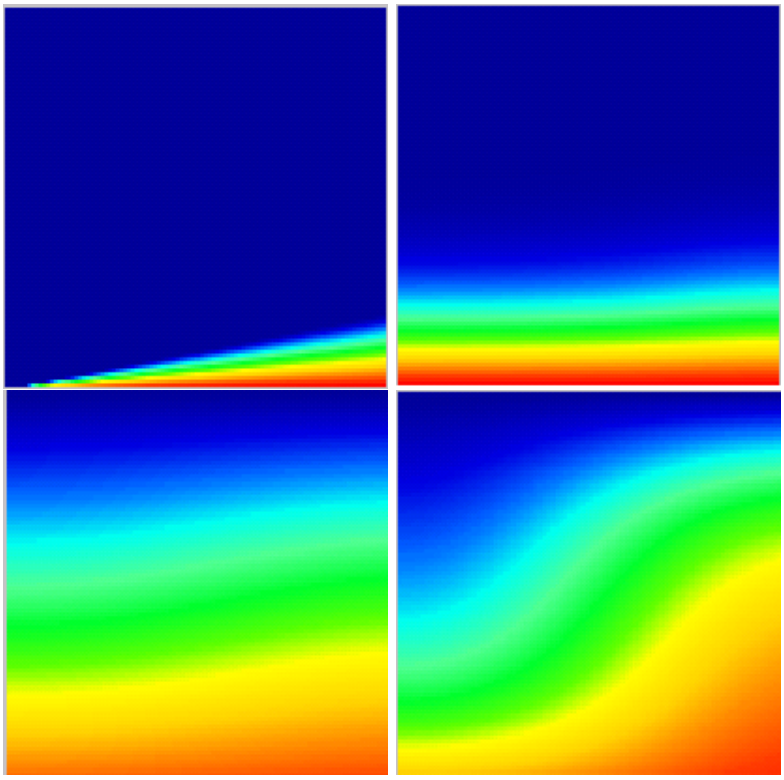

FIGURE 5.6. Mole fractions for a small Ra_c.

It is known that the fluid system is stable for a small Ra_c and it becomes unstable when Ra_c gets larger. In Fig. 5.6, the mole fractions are obtained with a small $Ra_c = 9.78$, and in Fig. 5.7, they correspond to a large $Ra_c = 978$. We have observed that for the present example instability occurs as $Ra_c \geq 40$.

5.4. Example 3. In the final example a mixture of six components (components: C_1, C_2, ..., C_6) is studied. They initially fill a rectangular reservoir with the heaviest component at the top of this reservoir (see the first figure in Fig. 5.8, where the blue color is the lightest), with molecular weights in the range 16.04, 36.37, 66.90, 121.97, 209.44, and 349.49. Other critical property data are given in Table 5.1, where a_c, ω_a, and ω_b are the acentric factor and EOS parameters for each component, and the binary interaction parameters are given in Table 5.2. No-flow boundary conditions are used for all equations. During the process of reaching equilibrium in an ultimate horizontal position, instability occurs at the interface of any two components (Fig. 5.8). Our nonlinear numerical simulation clearly shows the existence of multiple unstable interfaces. This is the first time to observe such a phenomenon for a fluid mixture of multiple components when the Peng-Robinson equations of state and the Lohrenz viscosity correlation are used in the compositional study. A major deficiency of current compositional commercial codes used to simulate gas injection is their failure to model the effect of unstable displacements caused either by adverse mobility ratios or by multicomponent gravity segregation.

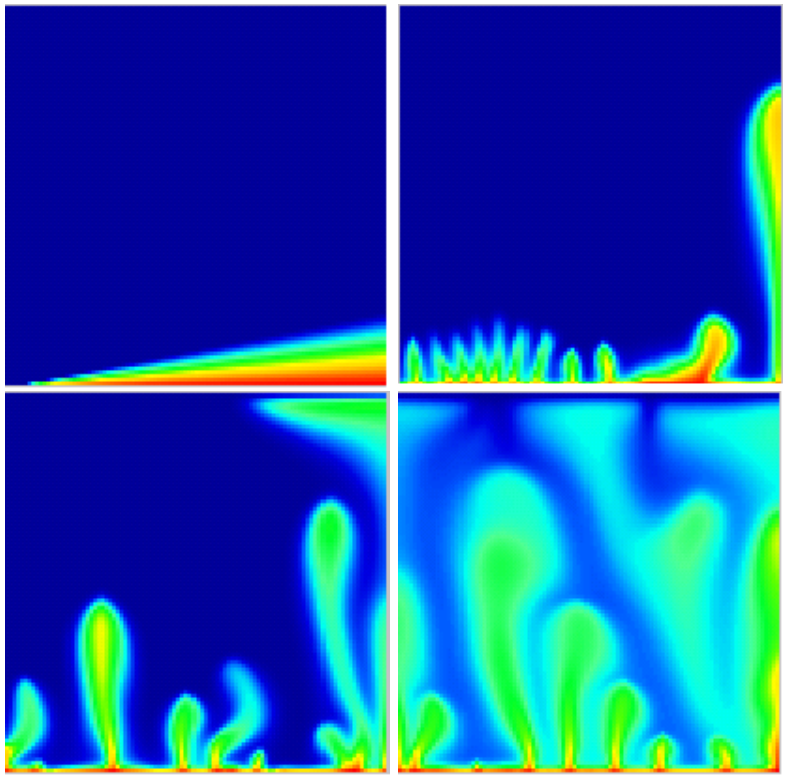

FIGURE 5.7. Mole fractions for a large Ra_c.

TABLE 5.1. Critical property data for Example 3.

T_c (F)	-115.78	133.28	353.74	655.19	874.55	1130.59
p_c (psi)	673.10	684.02	514.52	426.90	260.72	164.33
Z_c	0.28980	0.28103	0.27069	0.27192	0.23750	0.20873
W	16.04	36.37	66.90	121.97	209.44	349.49
a_c	0.00800	0.12465	0.22692	0.35436	0.55555	0.83181
ω_a	0.45723552	0.46571033	0.46630977	0.59811429	0.40070859	0.39639026
ω_b	0.07779607	0.07933397	0.07891004	0.10686607	0.05566172	0.06999792

TABLE 5.2. Binary interaction parameters for Example 3.

	C_1	C_2	C_3	C_4	C_5	C_6
C_1	0.000000	0.000112	0.006113	0.039906	0.048827	0.055951
C_2	0.000112	0.000000	0.007478	0.009804	0.009804	0.009804
C_3	0.006113	0.007478	0.000000	0.000000	0.000000	0.000000
C_4	0.039906	0.009804	0.000000	0.000000	0.000000	0.000000
C_5	0.048827	0.009804	0.000000	0.000000	0.000000	0.000000
C_6	0.055951	0.009804	0.000000	0.000000	0.000000	0.000000

The present study will provide a fundamental basis for correctly incorporating the effect of unstable displacements in the multiphase, multicomponent compositional simulators [3].

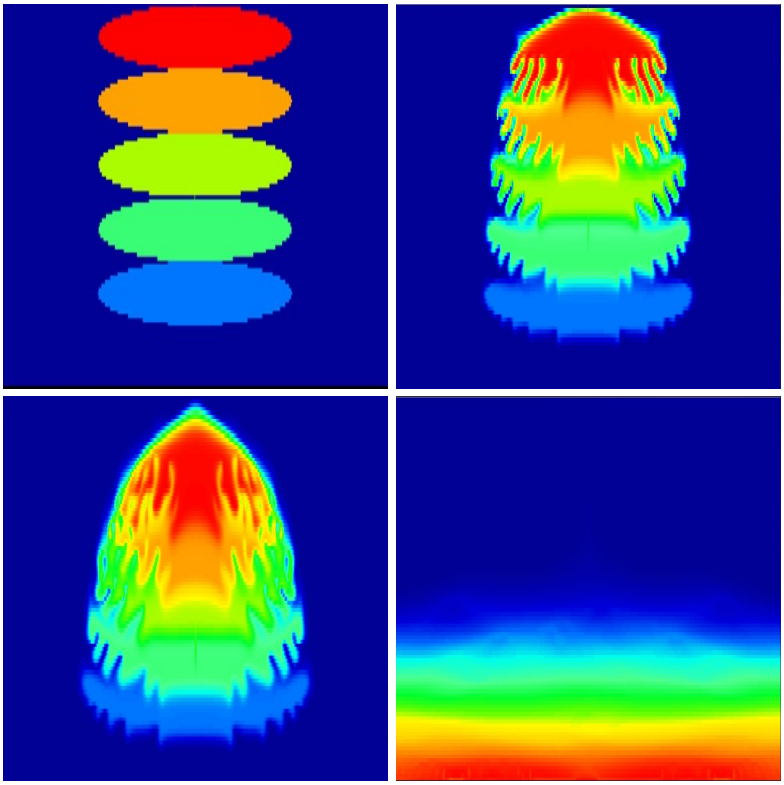

FIGURE 5.8. Mole fractions of Example 3 at different times.

6. Concluding Remarks

In this paper numerical simulation of multicomponent fluid mixing in porous media is presented. The effects of advection, diffusion, and gravity segregation to predict the development of compositional gradients in petroleum columns are studied. Special attention is paid to the gravity segregation for multiple components and the associated instability problem. The particular features of this fluid mixing simulator is that the primary unknowns are properly chosen so a conservative scheme can be designed, a finite volume method is used in the space discretization so flexible and adaptive grids can be adopted, and an adaptive time stepping technique is utilized so large time steps are possible while accuracy is preserved. The future work is to study the effects of pressure and thermal diffusion effects and extend the single phase, multicomponent fluid mixing to the multiphase, multicomponent case.

Acknowledgments. The authors would like to thank Drs. Changrui Gong, Guanren Huan, Wenjun Li, and Joe Zhou for their assistance in coding the fluid mixing simulator.

Nomenclature

Symbol	Quantity	Unit
c_b	Bulk specific heat capacity	$L^2/(Tt^2)$, Btu/(lbm-R) (J/(kg-K))
c_p	Fluid heat capacity	$L^2/(Tt^2)$, Btu/(lbm-R) (J/(kg-K))
$\mathbf{D}_{ij}^M$	Molecular diffusion coefficient	L^2/t, ft^2/D (m^2/d)
$\mathbf{D}_i^p$	Pressure diffusion coefficient	L^3t/M, $ft^2/(D\ psi)$ ($m^2/(d\ kPa)$)
$\mathbf{D}_i^T$	Thermal diffusion coefficient	$L^2/(tT)$, $ft^2/(D\ R)$ ($m^2/(d\ k)$)
D	Diffusion/dispersion	L^2/t, ft^2/D (m^2/d)
F	Function of viscosity	dimensionless
g	Gravitational acceleration	L/t^2, ft/D^2 (m/d^2)
$\mathbf{J}_i$	Diffusion/dispersion of component i	M/L^2t, $lbm/(ft^2D)$ kg·mole/(m^2d)
$\mathbf{k}$	Permeability tensor	L^2, darcy (μm^2)
k	Permeability	L^2, darcy (μm^2)
k_h	Horizontal permeability	L^2, darcy (μm^2)
k_T	Bulk thermal conductivity	$ML/(Tt^3)$, Btu/(ft-D-R) (J/(m-d-K))
k_v	Vertical permeability	L^2, darcy (μm^2)
N_c	Number of components	dimensionless
p	Pressure	$M/(Lt^2)$, psi (kPa)
q_i	Source/sink of component i	$M/(L^3t)$, $lbm/(ft^3D)$ kg·mole/(m^3d))
q_T	Heat source/sink	$M/(Lt^3)$, Btu/(ft^3D) (J/(m^3d))
r_i	Partial molar density of component i	mole/L^3, mole/ft^3 (mole/m^3)
T	Temperature	T, R (K)
t	Time	t, D (d)
$\mathbf{u}$	Darcy's velocity of fluid	L/t, ft/D (m/d)
W	Molecular weight	M/mole
W_i	Molecular weight of component i	M/mole
$\mathbf{x}$	Spatial variable (x_1, x_2, x_3)	L, ft (m)
$\mathbf{x}$	Mole vector	mole
x_i	Mole fraction of component i	fraction
z	Depth	L, ft (m)
μ	Viscosity of fluid	M/(Lt), cp (Pa·s)
ξ	Molar density of fluid	mole/L^3, mole/ft^3 (mole/m^3)
ϕ	Porosity	fraction
ρ	Fluid density	M/L^3, lbm/ft^3 (kg/m^3)
ρ_b	Bulk density	M/L^3, lbm/ft^3 (kg/m^3)
$\frac{\partial}{\partial t}$	Time derivative	t^{-1}, D^{-1} (d^{-1})
$\frac{\partial}{\partial x_i}$	Spatial derivative	L^{-1}, ft^{-1} (m^{-1})
$\frac{\partial^2}{\partial x_i^2}$	2nd spatial derivative	L^{-2}, ft^{-2} (m^{-2})
∇	Gradient operator	L^{-1}, ft^{-1} (m^{-1})
$\nabla\cdot$	Divergence operator	L^{-1}, ft^{-1} (m^{-1})
Δ	Laplacian operator	L^{-2}, ft^{-2}

References

[1] Z. Chen, Reservoir Simulation: Mathematical Techniques in Oil Recovery, the CBMS-NSF Regional Conference Series in Applied Mathematics, Vol. 77, SIAM, Philadelphia, PA, 2007.

[2] Z. Chen, G. Huan, and B. Li, An improved IMPES method for two-phase flow in porous media, *Transport in Porous Media* **54** (2004), 361–376.

[3] Z. Chen, G. Huan, and Y. Ma, Computational Methods for Multiphase Flows in Porous Media, in the Computational Science and Engineering Series, Vol. 2, SIAM, Philadephia, PA, 2006.

[4] Z. Chen, G. Zhou and D. Carruthers, Numerical simulation of compositional flow in porous media under gravity, *Communications in Computational Physics* **1**(2006), 827–846.

[5] Z. Chen and Y. Zhang, Development, analysis and numerical tests of a compositional reservoir simulator, *International Journal of Numerical Analysis and Modeling* **4** (2008), 86–100.

[6] K.-T. Chiang, Effect of a non-uniform basic temperature gradient on the onset of Bénard-Marangoni convection: Stationary and oscillatory analyses, *International Communications in Heat and Mass Transfer* **32** (2005), 192–203.

[7] K. Ghorayeb and A. Firoozabadi, Molecular, pressure, and thermal diffusion in nonideal multicomponent mixtures, *AIChE Journal* **46** (2000), 883–891.

[8] J. Gibbs, On the equilibrium of heterogeneous substances, *Trans. Conn. Acad.* **3** (1876), 108–248.

[9] G. M. Homsy, Viscous fingering in porous media, *Annu. Rev. Fluid Mech.* **19** (1987), 271–.

[10] D. Jacqmin, Interaction of natural convection and gravity segregation in oil/gas reservoirs, *SPE RE* May 1990, 233–238.

[11] M. Karimi, M. C. Charrier-Mojtabi, and A. Mojtabi, Onset of stationary and oscillatory convection in a tilted porous cavity saturated with a binary fluid: Linear stability analysis, *Physics of Fluids* **11** (1990), 1346–1358.

[12] J. Lohrenz, B. Bray, and R. Clark, Calculating viscosities of reservoir fluids from their compositions, *JPT* October 1964, 1171–1176.

[13] R. D. Moser, Mass transfer by thermal convection and diffusion in porous media, Paper presented at the 1986 International Conference on Applied Mechanics, Oct. 1986.

[14] M. Muskat, Distribution of non-reacting fluids in the gravitational field, *Physical Review* **35** (1930), 1384–1393.

[15] H. Nasrabadi, K. Ghorayeb, and A. Firoozabadi, Two-phase multicomponent diffusion and convection for reservoir initialization, *SPE REE* **9** (2006), 530–542.

[16] L. Onsager, Reciprocal relations in irreversible processes: I, *Phys. Rev.* **37** (1931), 405–426.

[17] L. Onsager, Reciprocal relations in irreversible processes: II, *Phys. Rev.* **38** (1931), 2265–2279.

[18] A. Peneloux, E. Rauzy, and R. Freze, A consistent correction for Redlich-Kwong-Soave volumes, *Fluid Phase Equilibria* **8** (1982), 7–23.

[19] D.-Y. Peng and D. B. Robinson, The characterization of the Heptanes and Heavier fractions for the GPA Peng-Robinson programs, *GPA Research Report*, RR–28, 1978.

[20] A. Riaz and E. Meiburg, Three-dimensional miscible displacement simulations in homogeneous porous media with gravity override, *J. Fluid Mech.* **494** (2003), 95–117.

[21] B. H. Sage and W. N. Lacey, Gravitational concentration gradients in static columns of hydrocarbon fluids, *Trans. AIME* **132** (1938), 120–131.

[22] A. M. Schulte, Compositional variations within a hydrocarbon column due to gravity, Paper SPE 9235 presented at the 1980 SPE Annual Technical Conference and Exhibition, Dallas, Sept. 21–24, 1980.

[23] H. Tchelepi and F. M. Orr, Jr., Interaction of viscous fingering, permeability heterogeneity, and gravity segregation in three dimensions, *SPE Reserv. Eng.* (November) 1994, 266–271.

[24] C. H. Whitson and P. Belery, Compositional gradients in petroleum reservoirs, SPE 28000, paper presented at the University of Tulsa Centennial Petroleum Engineering Symposium, Tulsa, August 1994.

Center for Computational Geoscienes, Faculty of Science, Xi'an Jiaotong University, Xi'an,710049, P.R. China. Department of Chemical & Petroleum Engineering, Schulich School of Engineering, University of Calgary, 2500 University Drive N.W. Calgary, Alberta, Canada T2N 1N4.
E-mail: zhachen@ucalgary.ca

Department of Chemical & Petroleum Engineering, Schulich School of Engineering, University of Calgary, 2500 University Drive N.W. Calgary, Alberta, Canada T2N 1N4.
E-mail: hchenyz@yahoo.com